Optical study of the vibrational and dielectric properties of $BiMnO_3$

W. S. Mohamed,[1] A. Nucara,[2] G. Calestani,[3] F. Mezzadri,[3] E. Gilioli,[4] F. Capitani,[1] P. Postorino,[1] and P. Calvani[2]

[1]*Dipartimento di Fisica, Università di Roma "La Sapienza", Piazzale A. Moro 2, 00185 Roma, Italy*

[2]*CNR-SPIN and Dipartimento di Fisica, Università di Roma "La Sapienza", Piazzale A. Moro 2, 00185 Roma, Italy*

[3]*Dipartimento di Chimica, Università di Parma, Parco Area delle Scienze 17A, 43124 Parma, Italy*

[4]*CNR-IMEM, Parco Area delle Scienze 37A, 43124 Parma, Italy*

(Received 3 June 2015; revised manuscript received 20 July 2015; published 24 August 2015)

$BiMnO_3$ (BMO), ferromagnetic (FM) below $T_c \simeq 100$ K, was believed to also be ferroelectric (FE) due to a noncentrosymmetric $C2$ structure, until diffraction data indicated that its space group is the centrosymmetric $C2/c$. Here we present infrared phonon spectra of BMO, taken on a mosaic of single crystals, which are consistent with $C2/c$ at any $T > 10$ K, as well as room-temperature Raman data which strongly support this conclusion. We also find that the infrared intensity of several phonons increases steadily for $T \to 0$, causing the relative permittivity of BMO to vary from 18.5 at 300 K to 45 at 10 K. At variance with FE materials of the displacive type, no appreciable softening has been found in the infrared phonons. Both their frequencies and intensities, moreover, appear insensitive to the FM transition at T_c.

DOI: 10.1103/PhysRevB.92.054306 PACS number(s): 77.80.−e, 78.30.Hv, 63.20.−e

I. INTRODUCTION

The possible multiferroicity—or, more precisely, magnetoelectricity—of $BiMnO_3$ (BMO), namely the simultaneous occurrence of ferroelectric (FE) and ferromagnetic (FM) long-range order in this simple perovskite, has been long discussed in the literature [1–5]. Such interest is justified by its potential applications, which may span from giant electric transformers and multiple-state memory elements, to spintronics, magnetoelectric sensors, electric-field controlled ferromagnetic devices, and variable transducers [6–11]. Indeed, on one hand, $BiMnO_3$ is ferromagnetic below [12,13] $T_c \simeq 100$ K, due to superexchange along the Mn^{3+}-$O^{2-}Mn^{3+}$ chains, with a maximum reported magnetization of 3.92 μ_B per formula unit [13,14]. On the other hand, the Bi^{3+} ($6\,s^2$) lone pair could experience a repulsion from the $2p$ orbitals of neighboring oxygen ions, leading to a permanent electric dipole and a ferroelectric distortion of the perovskite unit cell. However, both the detection of ferroelectricity and the observation of such distortion have long been controversial also due to the difficulty to grow single crystals [15] of BMO, since it is metastable at ambient pressure [14]. Indeed, the observation of ferroelectricity has been reported for thin films only [16,17], where moreover the results strongly depend on their thickness and oxygen stoichiometry [18].

Concerning bulk BMO, it has two structural phase transitions [13], i.e., at 470 K from monoclinic to monoclinic, and at 770 K from monoclinic to orthorhombic. Both first-principles calculations [7] and an experimental study [19] supported the FE hypothesis and were consistent with early diffraction studies, which identified a noncentrosymmetric $C2$ space-group symmetry [19,20]. However, recent experimental studies agree that the symmetry of the whole monoclinic phase at ambient pressure is the centrosymmetric $C2/c$ [14,21–23]. This excludes a ferroelectric phase for BMO, of the displacive type [24] at least. However, according to a recent model, inversion symmetry breaking might occur also in the $C2/c$ structure, due to some antiferromagnetic order hidden within canted ferromagnetism [25]. Finally, it was found that for increasing pressure, in single crystals, the symmetry evolves to the monoclinic $P2_1/c$ at 1 GPa and to the orthorhombic $Pnma$ at 6 GPa [23].

Valuable information on the crystal symmetry of an insulator can also be provided by optical studies (Raman and/or infrared) of its phonon spectrum. A factor group analysis gives for $C2$ the representation $29A + 31B$, where 57 phonons are both infrared (IR) and Raman active, while one A and two B vibrations are acoustic. In the space group $C2/c$, instead, the representation is $14A_g + 14A_u + 16B_g + 16B_u$ where, due to the inversion symmetry, all of the A_g and B_g modes are Raman active, the 13 A_u and 14 B_u modes are infrared active, and the remaining ones are acoustic. Previous infrared measurements of the BMO phonon spectrum [26] were fit to the sum of 32 Lorentzian modes. This number is higher than that predicted for the $C2/c$ space group (27), even if it is still much lower than that expected for the $C2$ symmetry (57).

To check and possibly solve this apparent contradiction, we have investigated the far-infrared reflectivity of a $BiMnO_3$ mosaic of small single crystals between 10 and 300 K. The resulting optical conductivity could be very well fit at 10 K to a sum of 25 Lorentzians, thus reconciling the results of infrared spectroscopy with a centrosymmetric structure for BMO. Moreover, we have taken Raman spectra on a single crystal belonging to the same mosaic, finding out that most of the 16 lines observed therein do not coincide with the infrared ones. This provides further support to the centrosymmetric structure $C2/c$, which is also consistent with the observation that no infrared line softens appreciably for $T \to 0$, as it would occur in displacive ferroelectricity. Finally, we observe a remarkable increase in the infrared oscillator strength for lowering temperature, which causes the extrapolated relative permittivity to increase smoothly from 18.5 at 300 K to 45 at 10 K.

II. EXPERIMENT AND RESULTS

The $BiMnO_3$ sample was grown and characterized as described in Ref. [23]. The compound was synthesized by a

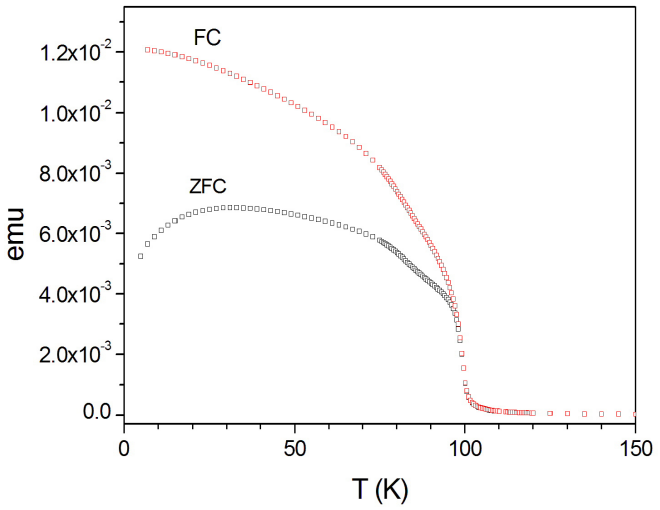

FIG. 1. (Color online) Magnetization vs temperature (in electromagnetic units, emu) of a single crystal extracted from the mosaic used for the infrared reflectivity measurements. The sample was cooled either in zero field (ZFC) or in a field of 100 oersted (FC). A sharp and single FM transition occurs at $T_c = 100$ K.

solid-state reaction of Bi_2O_3 (Aldrich 99.99%) and Mn_2O_3 (Aldrich 99.999%), with the latter one in slight excess, at 4 GPa and 1073 K, using a high-pressure multianvil apparatus to stabilize the phase. We thus obtained a mosaic, whose dimensions are about $5 \times 4 \times 1.5$ mm, made of single crystals too small to be used individually for the far-infrared measurements. Some of them were then extracted to perform the structural and magnetic measurements, while the rest of the batch was polished with powders having grain size down to 0.5 μm for the infrared experiment. Typical magnetization curves in field cooling (FC, 100 Oe) and zero-field cooling (ZFC) are shown in Fig. 1. They display a single and sharp FM transition at 100 K, which demonstrates the good chemical quality of the sample.

The sample reflectivity $R(\omega)$ was measured by an interferometer Bruker 66V, coupled to an Infrared Laboratories liquid-He cooled bolometer, a Hg-Cd-Te detector, or a Si photodiode, depending on the spectral range, with a spectral resolution of 2 cm^{-1} in the phonon region. The radiation was unpolarized: even if the whole sample were a single crystal, the monoclinic structure of BMO would prevent the obtainment of more meaningful information by polarized radiation. The sample temperature was regulated between 10 and 300 K with a thermal stability and accuracy of ± 2 K. The reference was a golden mirror close to the sample and oriented by a He-Ne laser parallel to it. Even if the region of interest is limited here to $50 \div 700$ cm^{-1}, the spectral range is extended from 30 to 10 000 cm^{-1} in order to obtain accurate Kramers-Kronig (KK) transformations [27]. The extrapolation from $\omega = 30$ cm^{-1} to $\omega = 0$ was performed by a constant $R(\omega)$, as usual for good insulators, the extrapolation to $\omega = \infty$ by a ω^{-4} power law [28]. The Raman spectra were measured with a Horiba LabRAM HR Evolution microspectrometer in backscattering geometry. The samples were different small crystals belonging to an unpolished area of the same mosaic where the infrared spectra were measured. They were excited by the 632.8 nm

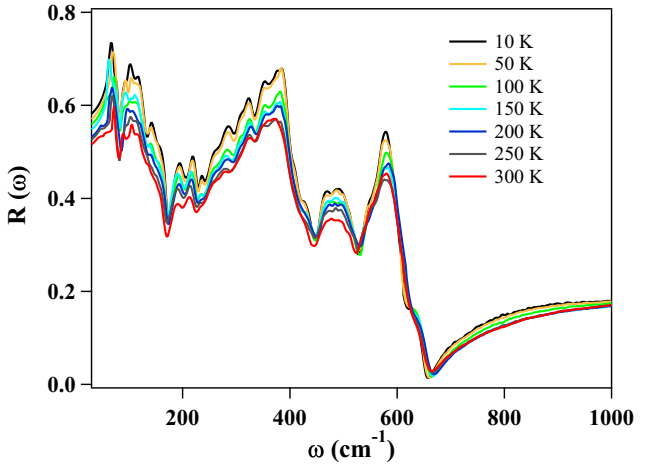

FIG. 2. (Color online) Reflectivity spectra of bulk $BiMnO_3$ in the far-infrared range of frequencies at different temperatures.

radiation of a He-Ne laser with 30 mW output power. The Raman spectra, like the infrared ones, were also taken in an unpolarized configuration. The detector was a Peltier-cooled charge-coupled device (CCD) and the resolution was 1 cm^{-1}, thanks to a 1800 grooves/mm grating with 800 mm focal length. Measurements were performed with a 20× objective (numerical aperture NA = 0.35).

The reflectivity of $BiMnO_3$ is shown in Fig. 2 in the far-infrared range at all temperatures and is basically similar to that reported in Ref. [26], including a strong increase of the intensity of some lines for $T \to 0$. Above that range, $R(\omega)$ looks flat and basically independent of temperature within the errors.

The optical conductivity $\sigma(\omega)$ extracted by the KK transformations from $R(\omega)$ is shown in Fig. 3. The phonon parameters were obtained by fitting $\sigma(\omega)$ to the sum of Lorentzian

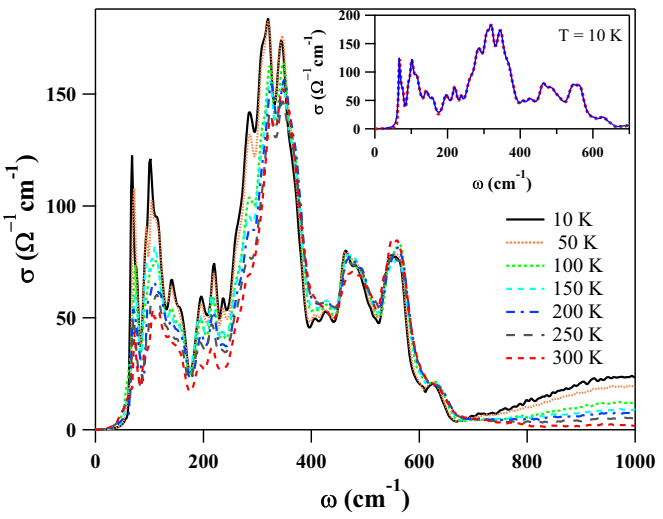

FIG. 3. (Color online) Optical conductivity of bulk $BiMnO_3$ in the far-infrared range, at different temperatures. Inset: The fit (dotted line) to the optical conductivity data (solid line) used to obtain the parameters at 10 K listed in Table I.

TABLE I. Infrared phonon frequencies Ω_j, oscillator strengths S_j, and widths Γ_j, as obtained by fitting to Eq. (1) the experimental $\sigma(\omega)$ at 10 and 300 K. All frequencies and widths are in cm^{-1}; intensities are in cm^{-2}.

Phonon (j)	Ω_j (10 K)	S_j(10 K)	Γ_j (10 K)	Ω_j (300 K)	S_j (300 K)	Γ_j (300 K)
1	68	39000	6	72	19000	8
2	75	30000	10			
3	92	21000	9	92	20000	16
4	101	60000	12	105	16000	11
5	115	100000	23	117	50000	24
6	143	54000	21	139	44000	31
7	159	26000	16	157	19000	20
8	196	57000	22	192	17000	18
9	219	49000	17	216	32000	24
10	237	12000	10	235	3000	12
11	261	78000	29	260	39000	32
12	284	178000	30	280	42000	31
13	308	115000	22	304	76000	38
14	321	90000	18	321	80000	24
15	345	230000	30	346	120000	50
16	369	110000	31	371	100000	44
17	407	7500	12			
18	426	56000	34	421	40000	46
19	463	80000	28	462	39000	30
20	486	110000	35	489	60000	45
21	508	48000	38			
22	541	47000	22	545	46000	25
23	561	125000	35	565	122000	39
24	604	3000	46			
25	628	18000	26	629	10000	28

oscillators,

$$\sigma_1(\omega) = \frac{1}{60}\sum_{j=1}^{n}\frac{\omega^2\Gamma_j S_j}{\left(\Omega_j^2-\omega^2\right)^2+\omega^2\Gamma_i^2}, \qquad (1)$$

where the factor $1/60$ allows for $\sigma_1(\omega)$ being measured [29] in $\Omega^{-1}\,cm^{-1}$. Here, Ω_j and Γ_j are the peak frequency and the linewidth of the jth transverse optical mode, respectively, in cm^{-1}, and S_j is the oscillator strength in cm^{-2}. The fitting parameters are listed in Table I for both the highest and the lowest temperature. Excellent fits (such as that shown in the inset of Fig. 3) were obtained at 10, 100, and 150 K for $n = 25$ oscillators, confirming the diffraction result that no structural change is associated with the FM transition. At 300 K, due to line broadening which superimposes some modes, only 21 oscillators were necessary. As already mentioned, in Ref. [26], the infrared phonon spectrum was fit using $n = 32$ modes instead, a value not compatible with the centrosymmetric $C2/c$. This discrepancy was tentatively explained by the authors in terms of overtones or combination bands—which, however, should have intensities much lower than the main lines, for the usual values of the anharmonic potential. The fact that here we get accurate fits down to 30 cm^{-1} for $n = 25$, i.e., a number of modes smaller than the 27 predicted for the centrosymmetric structure $C2/c$, makes our results consistent with those of diffraction [14,21,22].

According to well-known selection rules, the modes which are infrared active in a centrosymmetric structure are not Raman active, and vice versa. Therefore, to further check the BMO cell symmetry, we examined the Raman spectra of three microcrystals, which gave the same results. The experiment was done at room temperature, considering that diffraction data exclude phase transitions below 300 K [23], and that neither the Raman lines in Ref. [22] nor the infrared modes in Table I display major frequency shifts down to the lowest temperatures. A typical Raman spectrum is shown in Fig. 4, where 16 lines are observed, out of the predicted 30. Three of them, at or above 400 cm^{-1}, are poorly resolved. The data are very similar to those reported for room temperature in Ref. [22], but thanks to a somewhat larger experimental range, we observe an additional sharp line at 51 cm^{-1}. In the same Fig. 4, we also report the best resolved infrared spectrum of the mosaic in Fig. 3, that at 10 K. The two spectra look quite different and, except for a few features where the finite linewidths do not allow for a certain claim, the Raman lines do not coincide with the infrared ones. The Raman phonon frequencies and widths, obtained by fitting to data a sum of Lorentzians, are listed in Table II, which also allows for a comparison with the IR frequencies in Table I at 300 K. These results provide further support for our previous conclusion that the ions of BMO vibrate in a centrosymmetric cell.

Another interesting feature of the spectra in Fig. 3 is their temperature dependence. The frequencies do not change appreciably with T, and no phonon softening is observed which may indicate displacive ferroelectricity—not even incipient as in $SrTiO_3$ [30]. Moreover, we do not observe any appreciable shift in the ω_j's around or below the FM transition. In

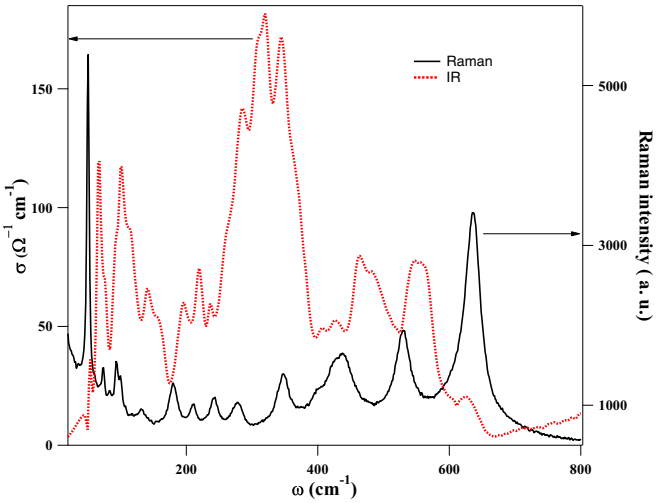

FIG. 4. (Color online) Raman spectrum of a single crystal of $BiMnO_3$ at room temperature and infrared spectrum of the mosaic at 10 K, extracted from Fig. 3. Given the weak T dependence observed in both spectra (see Table I and Ref. [22]), the best resolved IR spectrum has been chosen for a more meaningful comparison.

Ref. [22], a low-frequency shift was reported for the Raman bands at 513.8 and 637.4 cm^{-1} below T_c. The authors attribute this observation to a spin-phonon coupling which is switched on by the FM transition. The absence of a corresponding effect in the present infrared data indicates that such interaction, if able to change the Raman polarizability, does not appreciably affect the first-order interaction of the radiation with the lattice dipole moment.

However, as we already mentioned and is evident in Table I, the oscillator strengths S_j of some lines (with $j = 1$, 4, 5, 8, 11, 12, 15, 20, 25) increase by about a factor of two, or even more, from 300 to 10 K, an effect that can be observed also in Fig. 2 of Ref. [26]. Fits to our data at all temperatures

TABLE II. Raman phonon frequencies Ω_j obtained by fitting to Eq. (1) the $BiMnO_3$ Raman intensity at 300 K. All frequencies and widths are in cm^{-1}.

Phonon (j)	Ω_j (300 K)	Γ_j (300 K)
1	50	2
2	74	1
3	84	1
4	93	1
5	99	1
6	133	6
7	180	9
8	211	9
9	242	10
10	278	15
11	347	15
12	400	15
13	424	12
14	440	17
15	530	12
16	635	14

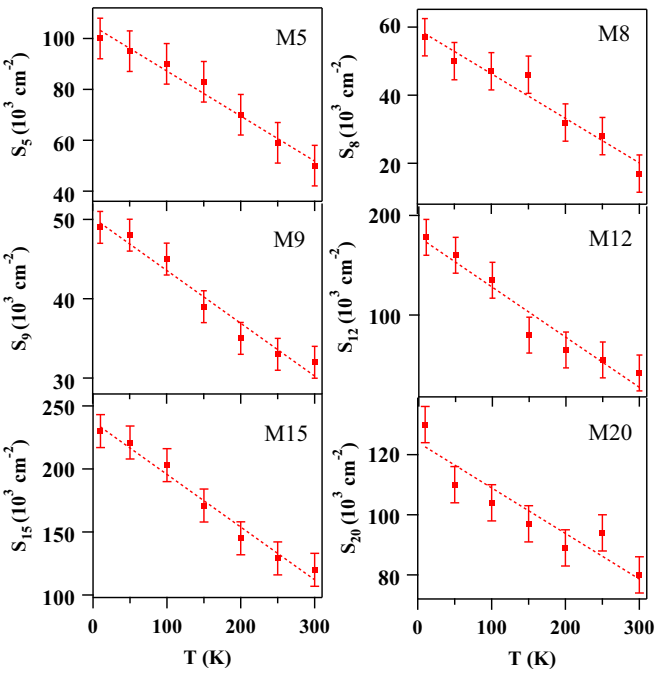

FIG. 5. (Color online) Systematic increase of the oscillator strength of $BiMnO_3$ phonons for $T \to 0$. The modes (M) are numbered as in Table I and the lines are guides to the eye. Within errors, no reproducible features are observed around the FM transition at $T_c \simeq 100$ K.

show that the intensity of those phonons linearly increases for decreasing temperature, as shown in Fig. 5, and is insensitive to the FM transition at T_c. Similar effects have been observed in several insulating oxides with high polarizability [31–34] and often attributed to the so-called charged-phonon effect [35] by which phonons acquire an anomalously large spectral weight due to a redistribution of electronic charge, within the cell, associated with their displacement pattern. Such increase of spectral weight in the far-infrared region causes the failure of the f-sum rule,

$$\int_0^{\omega_{\max}} \sigma(\omega, T) d\omega = \text{const}, \qquad (2)$$

if $\omega_{\max}$ does not include the regions where the transferred spectral weight comes from, presumably the electronic bands in the visible and the UV, which are out of the present measuring range. Anyway, checking such assumption would be a very hard task, given the small width of the far-infrared (FIR) range [where the spectral weight in Eq. (2) increases for lowering temperature] with respect to the spectral regions where it should decrease. The same holds for the weak band partially shown in Fig. 3, at frequencies higher than the phonon range. It can either result from an admixture of phonon overtones and combination bands, consistent with its low intensity, or have a polaronic origin, namely, coming from excess charges self-trapped in the lattice. Those charges could be related to oxygen nonstoichiometry, which is likely to occur in this oxide [36]. In both cases, the band intensity will increase for $T \to 0$: in the former one because it will follow the strengthening of the individual phonons, and in the latter

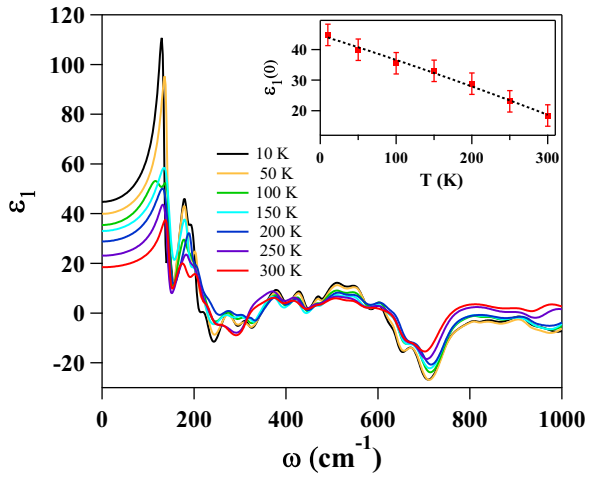

FIG. 6. (Color online) Behavior with frequency and temperature of the real part of the dielectric function $\epsilon_1(\omega)$ in $BiMnO_3$. Inset: The temperature dependence of its extrapolation to zero frequency, the (relative) dielectric constant $\epsilon_1(0)$.

one because, at low T, more quasifree charges will self-trap in the local distortions [37,38].

Together with the optical conductivity, which is related to the imaginary part of the dielectric function $\tilde{\epsilon}(\omega)$, the KK transformations provide its real part $\epsilon_1(\omega)$, which is shown in Fig. 6. If one assumes the absence of strong modes at frequencies lower than the limit of this experiment (30 cm^{-1}), its extrapolation to zero frequency gives the relative permittivity $\epsilon_1(0)$, which can thus be determined vs temperature without any metal deposition and contacts on the sample, which may affect the measurement. As shown in the inset of the same figure, due to the above-described growth of several phonon intensities at low T, it increases smoothly from 18.5 at 300 K to 45 at 10 K. These rather low values support once again the absence of a ferroelectric phase in $BiMnO_3$ down to 10 K.

III. CONCLUSION

In order to further investigate the possible occurrence of ferroelectricity in $BiMnO_3$, we have measured the infrared phonon spectrum of a mosaic of small single crystals from 300 to 10 K. We find that at the lowest T, it can be accurately fit by using only 25 Lorentz oscillators, out of the 27 predicted for the $C2/c$ symmetry that has been attributed to $BiMnO_3$ by the most recent diffraction experiments. To further check the conclusion that the BMO cell is centrosymmetric, we have measured the Raman spectrum at 300 K of three single crystals belonging to the mosaic, and we have observed 16 phonon lines out of the 30 predicted for $C2/c$. Most of them are definitely different from the infrared lines, while for a few others, the finite linewidths in both spectra do not allow for an unambiguous conclusion. This is consistent with a centrosymmetric structure such as $C2/c$, while, in the case of broken inversion symmetry, the Raman and infrared combs should substantially coincide. If one adds that our data do not show any appreciable phonon softening, the present results point consistently toward the absence of ferroelectricity—and therefore of multiferroicity—in $BiMnO_3$ down to 10 K, at least of the displacive type.

However, we observe a regular increase of the oscillator strength in several modes of $BiMnO_3$ for lowering temperature. This causes the extrapolation to zero frequency of the real part of the dielectric function, namely, the relative permittivity, to increase from 18.5 at 300 K to 45 at 10 K. Across the ferromagnetic transition at $T_c \simeq 100$ K, we do not detect any major anomaly in the oscillator strength or in the phonon frequency. Therefore, we conclude that the phonon-spin interaction recently invoked to interpret the behavior of a few Raman phonon lines does not affect the dipole moment which interacts at first order with the radiation field.

[1] N. Hur, S. Park, P. A. Sharma, S. Guha, and S.-W. Cheong, Phys. Rev. Lett. **93**, 107207 (2004).
[2] L. C. Chapon, G. R. Blake, M. J. Gutmann, S. Park, N. Hur, P. G. Radaelli, and S.-W. Cheong, Phys. Rev. Lett. **93**, 177402 (2004).
[3] M. Fiebig, Th. Lottermoser, D. Frohlich, A. V. Goltsev, and R. V. Pisarev, Nature (London) **419**, 818 (2002).
[4] M. Grizalez, G. A. Mendoza, and P. Prieto, J. Phys.: Conf. Ser. **167**, 012035 (2009).
[5] Th. Lottermoser, Th. Lonkai, U. Amann, D. Hohlwein, J. Ihringer, and M. Fiebig, Nature (London) **430**, 541 (2004).
[6] C. Binek and B. Doudin, J. Phys. Condens. Matter **17**, L39 (2005).
[7] N. A. Hill and K. M. Rabe, Phys. Rev. B **59**, 8759 (1999).
[8] W. Eerenstein, N. D. Mathur, and J. F. Scott, Nature (London) **442**, 759 (2006).
[9] A. A. Belik, J. Solid State Chem. **195**, 32 (2012).
[10] M. Fiebig, J. Phys. D **38**, R123 (2005).
[11] S. W. Cheong and M. Mostovoy, Nat. Mater. **6**, 13 (2007).
[12] F. Sugawara, S. Iiida, Y. Syono, and S. Akimoto, J. Phys. Soc. Jpn. **25**, 1553 (1968).
[13] T. Kimura, S. Kawamoto, I. Yamada, M. Azuma, M. Takano, and Y. Tokura, Phys. Rev. B **67**, 180401(R) (2003).
[14] E. Montanari, G. Calestani, L. Righi, E. Gilioli, F. Bolzoni, K. S. Knight, and P. G. Radaelli, Phys. Rev. B **75**, 220101 (2007).
[15] P. Toulemonde, C. Darie, C. Goujon, M. Legendre, T. Mendonca, M. lvarez-Murga, V. Simonet, P. Bordet, P. Bouvier, J. Kreisel, and M. Mezouar, High Press. Res. **29**, 600 (2009).
[16] A. Moreira dos Santos, S. Parashar, A. R. Raju, Y. S. Zhao, A. K. Cheetham, and C. N. R. Rao, Solid State Commun. **122**, 49 (2002).
[17] A. Sharan, J. Lettieri, Y. F. Jia, W. Tian, X. Q. Pan, D. G. Schlom, and V. Gopalan, Phys. Rev. B **69**, 214109 (2004).
[18] E. Montanari, L. Righi, G. Calestani, A. Migliori, E. Gilioli, and F. Bolzoni, Chem. Mater. **17**, 1765 (2005).

[19] A. Moreira dos Santos, A. K. Cheetham, T. Atou, Y. Syono, Y. Yamaguchi, K. Ohoyama, H. Chiba, and C. N. R. Rao, Phys. Rev. B **66**, 064425 (2002).
[20] T. Atou, H. Chiba, K. Ohoyama, Y. Yamaguchi, and Y. Syono, J. Solid State Chem. **145**, 639 (1999).
[21] A. A. Belik, S. Iikubo, T. Yokosawa, K. Kodama, N. Igawa, S. Shamoto, M. Azuma, M. Takano, K. Kimoto, Y. Matsui, and E. Takayama-Muromachi, J. Am. Chem. Soc. **129**, 971 (2007).
[22] P. Toulemonde, P. Bordet, P. Bouvier, and J. Kreisel, Phys. Rev. B **89**, 224107 (2014).
[23] G. Calestani, F. Orlandi, F. Mezzadri, L. Righi, M. Merlini, and E. Gilioli, Inorg. Chem. **53**, 8749 (2014).
[24] J. F. Scott, Rev. Mod. Phys. **46**, 83 (1974).
[25] I. V. Solovyev and Z. V. Pchelkina, Phys. Rev. B **82**, 094425 (2010).
[26] V. Goian, S. Kamba, M. Savinov, D. Nuzhnyy, F. Borodavka, P. Vank, and A. A. Belik, J. Appl. Phys. **112**, 074112 (2012).
[27] M. Dressel and G. Grüner, *Electrodynamics of Solids* (Cambridge University Press, Cambridge, 2002), p. 56.
[28] J. Yang, J. Hwang, T. Timusk, A. S. Sefat, and J. E. Greedan, Phys. Rev. B **73**, 195125 (2006).
[29] T. Timusk and T. Tanner, in *Physical Properties of High T_c Superconductors*, edited by D. M. Ginsberg (World Scientific, Singapore, 1989), p. 347.
[30] A. Yamanaka, M. Kataoka, Y. Inaba, K. Inoue, B. Hehlen, and E. Courtens, Europhys. Lett. **50**, 688 (2000), and references therein.
[31] C. C. Homes, T. Vogt, S. M. Shapiro, S. Wakimoto, and A. P. Ramirez, Science **293**, 673 (2001).
[32] C. C. Homes, T. Vogt, S. M. Shapiro, S. Wakimoto, M. A. Subramanian, and A. P. Ramirez, Phys. Rev. B **67**, 092106 (2003).
[33] P. Calvani, M. Capizzi, S. Lupi, and G. Balestrino, Europhys. Lett. **31**, 473 (1995).
[34] A. Nucara, W. S. Mohamed, L. Baldassarre, S. Koval, J. Lorenzana, R. Fittipaldi, G. Balakrishnan, A. Vecchione, and P. Calvani, Phys. Rev. B **90**, 014304 (2014).
[35] M. J. Rice, Solid State Commun. **31**, 93 (1979).
[36] D. W. Boukhvalov and I. V. Solovyev, Phys. Rev. B **82**, 245101 (2010).
[37] A. J. Millis, R. Mueller, and Boris I. Shraiman, Phys. Rev. B **54**, 5405 (1996).
[38] P. Calvani, Riv. Nuovo Cimento **24**, 1 (2001).